ECCOMAS Thematic Conference on Computational Methods
in Structural Dynamics and Earthquake Engineering
M. Papadrakakis, D.C. Charmpis, N.D. Lagaros, Y. Tsompanakis (eds.)
Rethymno, Crete, Greece, 13–16 June 2007

RETROFITTING OF BRIDGE HOLLOW PIERS WITH CFRP

Pedro Delgado[1*], Patrício Rocha[1], João Pedrosa[2], António Arêde[2], Nelson Vila Pouca[2], Miguel Santos[3], Anibal Costa[4], Raimundo Delgado[2]

[1] Polytechnic Institute of Viana do Castelo
Apartado 574, 4901-908 Viana do Castelo, Portugal
pdelgado@fe.up.pt, (pdelgado, procha)@estg.ipvc.pt

[2] Faculty of Engineering of University of Porto
R. Dr. Roberto Frias, s/n 4200-465 Porto, Portugal
(aarede, nelsonvp, rdelgado)@fe.up.pt

[3] S.T.A.P. – Reparação, consolidação e modificação de estruturas, S. A.
www.stap.pt

[4] Department of Civil Engineering, University of Aveiro
Campus Universitário de Santiago, 3810-193 Aveiro, Portugal
acosta@civil.ua.pt

Keywords: Experimental tests, Non-linear cyclic behavior, Numerical structural modelling, Seismic retrofit, Bridge piers, CFRP.

Abstract. *Hollow bridge piers generally have large section dimensions, with reinforcement bars spread along both wall faces. Unlike common solid section columns, quite often the shear effect has great importance on the pier behavior. Therefore, it is of particular relevance that special attention is given to this issue when the assessment and retrofit of RC hollow section piers is envisaged. Representative of typical bridge construction, RC piers were tested at LESE – the Laboratory of Earthquake and Structural Engineering of the Faculty of Engineering of University of Porto. Experimental tests of hollow section piers with square and rectangular cross sections under cyclic loading are being carried out in order to compare the results of the original piers and CFRP retrofitted piers, regarding benefits on their structural behavior and comparing the results with analytical predictions. The adopted numerical methodologies are based on finite element analysis using 3D elements with a Continuum Damage Mechanics model for the concrete under tensile and compressive reversals and truss elements with the Menegotto-Pinto model for the cyclic behavior of steel reinforcement. For different rectangular cross sections, the interaction between pier walls is likely to affect their global behavior and damage. The main purpose of this paper is therefore to present several strategies of retrofit with CFRP in order to prevent shear or flexural collapse mechanisms, or both. Different amounts of strip layers were applied for shear retrofit and jacket confinement near the pier base section was adopted for increasing ductility. It is intended to assess the structural behavior and safety improvement due to the adoption of different CFRP retrofit techniques and to illustrate the external and internal damage pattern. The need of interior retrofit is discussed on the basis of experimental evidence from some of the tests; therefore a strategy of internal confinement is also presented in order to prevent interior concrete spalling and longitudinal rebar buckling.*

1 INTRODUCTION

Bridges and viaducts are, amongst all the structures, those that sustain the most damage, as clearly demonstrated in several reports of recent earthquakes. In comparative terms, these consequences of bridge vulnerability are found greater than those observed in building structures and, in most cases, the bridge safety is limited and conditioned by pier capacities. Several studies and works have been carried out on solid piers and can be applied to building structures [1]; however, for hollow piers much less research is found in the literature. Usually, hollow piers have large section dimensions, with reinforcement bars spread along both wall faces. Unlike common solid section columns, quite often the shear effect has great importance on the pier behavior [2]. Therefore, it is of particular relevance that special attention is given to this issue when the assessment and retrofit of RC hollow section piers is envisaged.

The main purpose of this paper is to present an experimental campaign of reinforced concrete hollow section piers under cyclic loading in order to compare the results of the original piers with those obtained after CFRP seismic retrofit, to evaluate benefits concerning their structural behavior and to compare the results with analytical model. Rectangular RC hollow piers have a particular structural behavior, close to structural walls, and therefore are more difficult to simulate with simple numerical tools; this fact is indeed a strong motivation for this work. The adopted numerical methodology resorts to sophisticated constitutive models, simulating the non-linear cyclic behavior of the concrete by a constitutive model based on the Continuum Damage Mechanics and using 3D finite element discretizations for the concrete, while truss elements are used for the steel with a cyclic behavior model. Moreover, for different rectangular cross section dimensions, the interaction between the pier walls can strongly influence their global behavior and observed damage. Therefore, a set of rectangular hollow section RC piers, representative of typical bridge construction, were tested at LESE – the Laboratory of Earthquake and Structural Engineering of the Faculty of Engineering of University of Porto, [3][4]. The test setup was designed to impose cyclic horizontal top displacements with axial load and the possibility of using two orthogonal actuators with a sliding device that allows pier top displacements and rotations, relative to the vertical actuator fixed to a steel portal frame. The basic aim is, therefore, to contribute for the structural behavior and safety improvement assessment of different retrofit techniques adopted, while addressing the actually observed external and internal damage pattern. In addition, development and calibration is sought concerning analytical tools suitable for the evaluation of cyclic response of rectangular hollow piers.

2 EXPERIMENTAL CAMPAIGN

2.1 Testing setup

The test setup, shown in Figure 1, makes use of a 500 kN actuator to apply lateral loads and a 700 kN actuator to apply axial loads. The specimen and reaction frame are bolted to the strong floor with high strength prestressed rods. A constant axial load was applied during the tests, herein described, while the lateral loads were cycled, under displacement controlled conditions. A special sliding device consisting of two steel plates, shown in Figure 2, was used to minimize the friction created by the axial loads. The lower plate is bonded to the specimen top, whereas the upper is hinged to the vertical actuator, allowing top-end displacements and rotations on the specimens to take place when lateral loading is imposed during the test. The upper plate is also connected to a load cell to measure the residual frictional force between the two plates. During the tests, the hydraulic system of the vertical actuator was designed to keep constant the oil pressure, in order to maintain constant the axial force. The

horizontal actuator control is done using a PXI controller system from National Instruments (NI) and specifically home developed control routines based on the LabVIEW software platform (also from NI). The data acquisition is also based on another PXI system equipped with acquisition and signal conditioning cards and allows direct reading of data from strain gauges, load cells, LVDTs (Linear Voltage Displacement Transducers) and other types of amplified analogical or digital sensors.

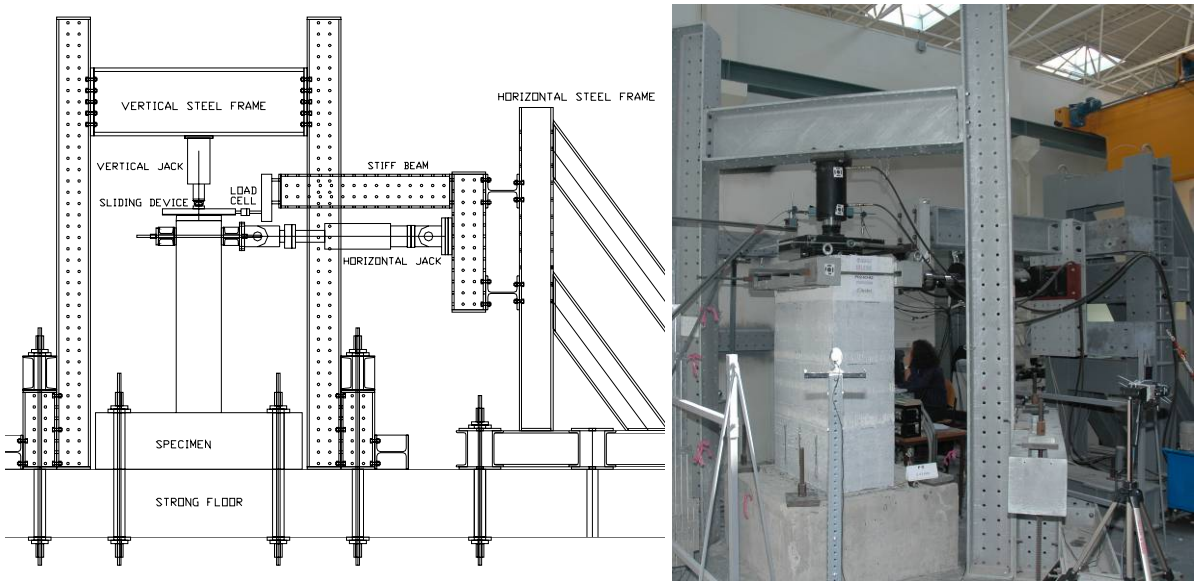

Figure 1: Schematic layout and view of the test setup at LESE laboratory.

Figure 2: The sliding device used to apply the axial load.

2.2 Specimens and Instrumentation

The specimens presented in this paper correspond to the second group of piers tested within this framework, being the results of the first group already shown in previous reports [3], [4]. This set of specimens, consisting on rectangular hollow section RC piers with 450mm x 900mm exterior dimensions and 75mm thick walls, was based on square piers tested at the Laboratory of Pavia University, Italy,[5] and is being tested in order to understand the influence of the cross section geometry of rectangular hollow piers on the cyclic behavior, bearing in mind the purpose of assessing retrofitting solutions. The unconfined concrete compressive strength is 35 MPa and for both longitudinal and transversal reinforcement the yielding strength is 450 MPa. The model schemes shown in Figure 3a correspond to ¼ scale representations of hollow section bridge piers, herein referred to as PO: PO1 for square section and PO2 for rectangular section. Instrumentation to measure curvature and shear deformations

was included along the pier height, because important shear deformations were expected in these tests. The LVDT configuration used in both specimens is shown in Figure 3b.

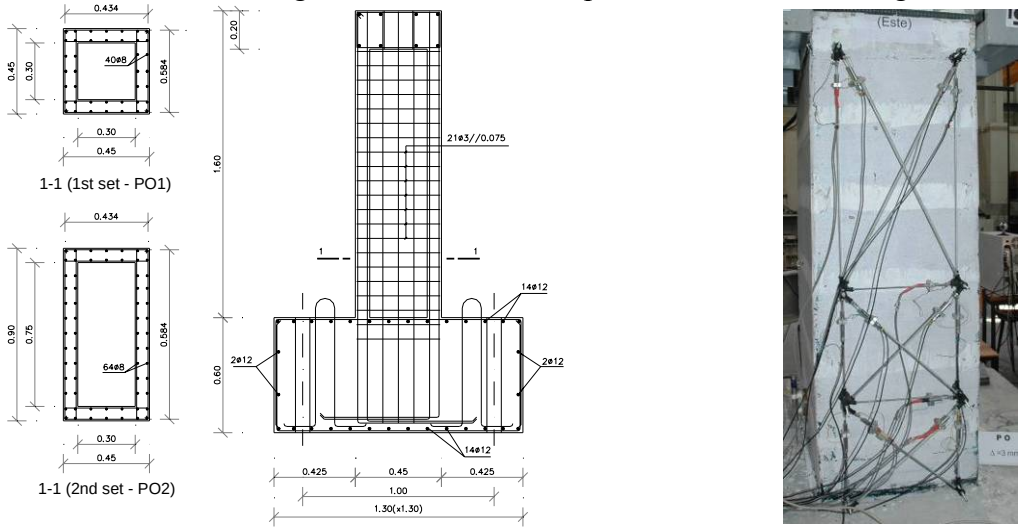

(a) (b)

Figure 3: Hollow RC piers: a) model schemes and b) lateral LVDT layout.

3 CYCLIC TESTS AND NUMERICAL ANALYSIS

Two original specimens were tested, namely the piers PO2-N2 and PO2-N3 under constant axial load of 250 kN and 440 kN, respectively. In order to characterize the piers cyclic behavior, three cycles were applied for each of the following peak drift ratios: 0.1%, 0.2%, 0.35%, 0.7%, 0.3%, 1.0%, 1.2%, 0.5%, 1.8%, 2.1% and 2.4%.

3.1 Pier damage

Concerning the test results of original specimens PO2-N2 and PO2-N3, the greatest amount of damage was mainly observed at the lateral sides, east and west, where the concrete cover crushed within the entire pier height (see Figures 4 and 5) and strong shear damage was achieved due to concrete degradation caused by lack of transverse reinforcement efficiency. Little damage was observed in the north and south sides, with well distributed cracks. However, the cracks observed in those sides are not only horizontal, as for the square piers tested before [4], but instead they show an angle that increases along the pier height, due the shear lag effect that occurs for this width/height ratio (2:1).

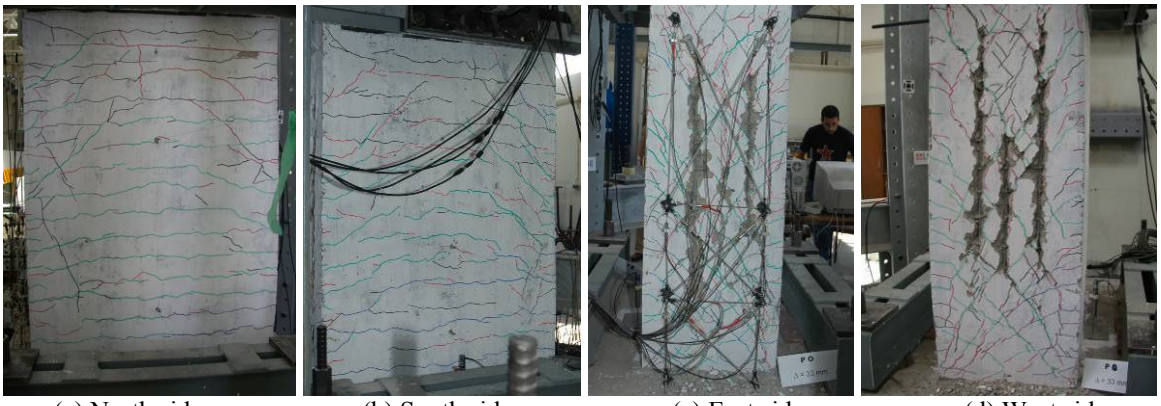

(a) North side (b) South side (c) East side (d) West side

Figure 4: Pier PO2-N2 damage for 2.4% drift.

(a) North side (b) South side (c) East side (d) West side

Figure 5: Pier PO2-N3 damage for 2.4% drift.

3.2 Cyclic results and numerical analysis

Figure 6a shows the experimental responses of both piers PO2-N2 and PO2-N3 in terms of top force-displacement diagrams; as expected, these diagrams show larger initial stiffness and maximum forces for the pier with higher axial load (PO2-N3). However, failure of both piers was reached by the first cycles of 25mm amplitude (1.8% drift), with visible shear failure mode and the shear lag effect evidenced in the damage pattern shown in Figures 4 and 5.

Concerning the numerical analysis for cyclic loading the CAST3M computer code [6] was adopted, a general purpose finite element based program, where a wide variety of non-linear behavior models are available and, particularly, a damage model developed at FEUP [7] and recently implemented in CAST3M [8], that has already proved to be suitable for seismic behavior analysis of RC bridge piers [9]. This later modeling strategy thus involves: the above mentioned Continuum Damage Mechanics based constitutive model for the concrete zone discretized into 3D finite elements and incorporating two independent scalar damage variables that account for the degradation induced by tensile or compressive stress conditions; the Giuffré-Menegotto-Pinto model [10] for the cyclic behavior simulation of the steel reinforcement discretized via truss elements. Results of the numerical model for pier PO2-N2 are included in Figures 6b and 7.

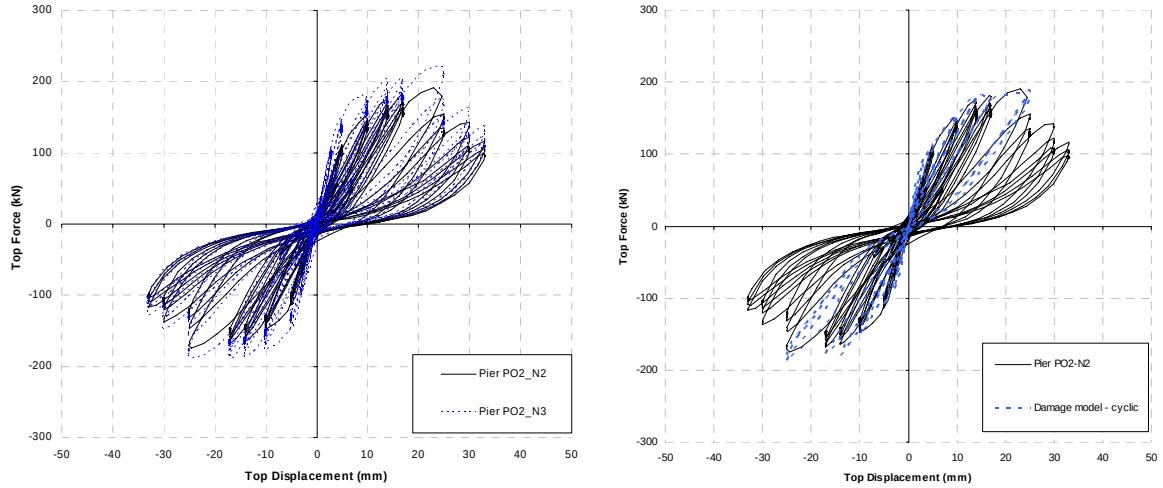

(a) Experimental comparison for PO2-N2 and PO2-N3 (b) Numerical analysis for pier PO2-N2

Figure 6: Experimental and numerical results comparison.

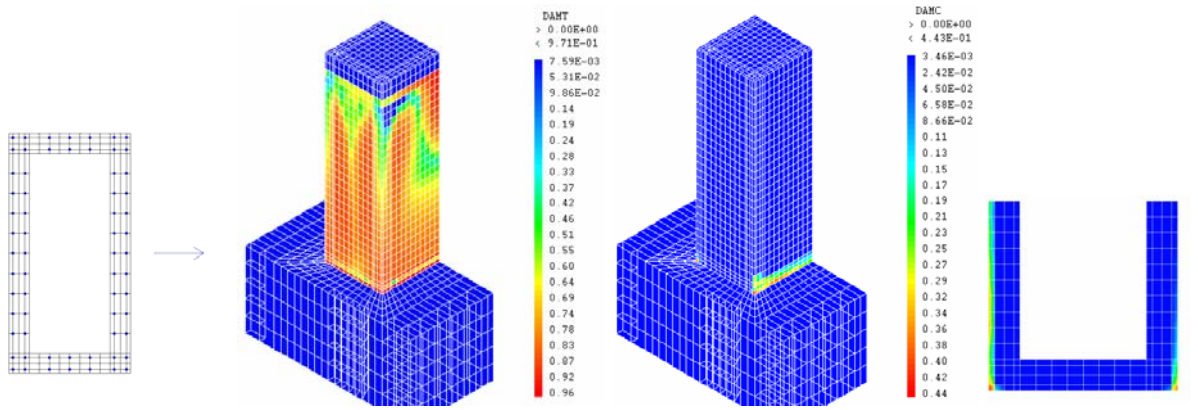

(a) Section discretization (b) Tensile damage for 5mm (c) Comp. damage for 25mm (d) Section comp. damage

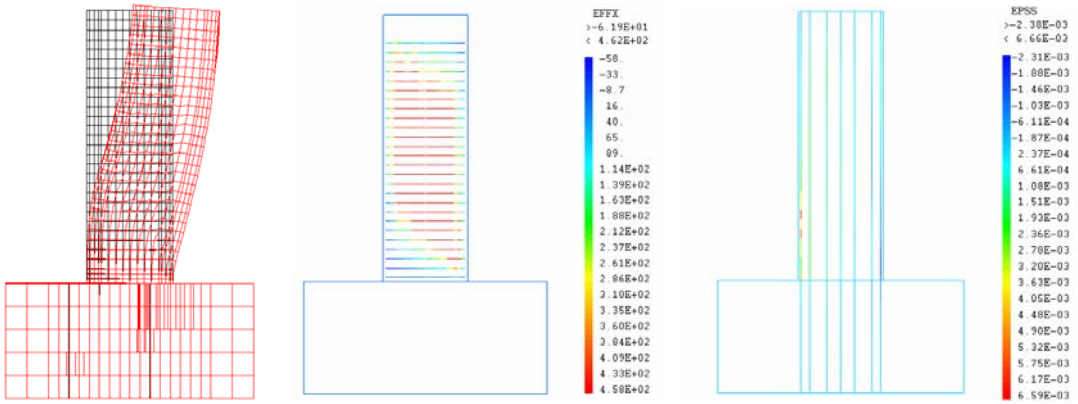

(e) Deformed mesh (f) Transverse reinf. strength (g) Longitudinal reinf. strain

Figure 7: Numerical results of PO2-N2 for 1.8% drift.

As already referred before, a shear failure mechanism was observed on the pier response; these effects were satisfactorily captured by the damage model as evidenced by the cyclic curves shown in Figure 6b. The 3D finite element discretization used in the damage model is shown in Figure 7a, but in fact only half of the cross section was modeled with adequate symmetry conditions. The result of tensile damage pattern is illustrated in Figure 7b for the initial cycles, around 5mm, where first cracks were found; the compressive damage pattern is also shown (Figures 7c and 7d) for 1.8% drift, where some damage is observed at the pier base. The deformed mesh for the horizontal displacement of 25mm (about 1.8% drift) is also included in Figure 7e. From the results shown in Figures 7f and 7g, it is possible to observe the stress and strain distribution, respectively, along the transversal and longitudinal reinforcement bars, for 1.8% drift, where steel yielding is evidenced in red. The transverse reinforcement stress pattern allows identifying the strut-and-tie shear mechanism development and the longitudinal rebar strain distribution shows yielding in the outer bars above the foundation.

With these numerical results it is possible to confirm the shear failure around the 25mm cycle, but with previous yielding of some longitudinal rebars near the pier base. When compared to the experimental tests, larger forces were obtained from numerical results, possibly due to more longitudinal rebars already within the yielding phase.

4 THE RETROFIT PROCESS

After the cyclic tests of the original specimens, they were repaired and retrofitted by an external contractor (S.T.A.P.) according to the following steps: 1) delimitation of the repair area; 2) removal and cleaning of the damaged concrete; 3) inside retrofit with transversal steel bars;

4) application of formwork and new concrete (Microbeton, a pre-mixed micro concrete, modified with special additives to reduce shrinkage in the plastic and hydraulic phase); 5) outside retrofit with the CFRP sheets. In order to provide a general idea of the pier damage and of the retrofit process, the following photographs show the piers during repair and after having been retrofitted with CFRP sheet jackets (Figure 8).

Figure 8: Hollow piers before and after the shear retrofitting with inside steel bars and outside CFRP sheet.

The inside transversal steel bars (only for pier PO2-N3-R2) were designed taking in account the feasibility for future real retrofits; such bars were concentrated at the bottom, in correspondence with the outer CFRP jackets, for improving the plastic hinge confinement. In order to design the outside shear retrofit with CFRP jackets, the authors adopted the Priestley approach [11] to evaluate the thickness of the rectangular hollow pier jacket for increasing the shear strength above the maximum flexural force while keeping the initial section conditions. According to Priestley methodology the shear strength can be conveyed by Eq. (1) [11]:

$$V_d = V_c + V_s + V_p + V_{sj} \tag{1}$$

where V_c, V_s and V_p are the shear force components accounting, respectively, for the nominal strength of concrete, the transverse reinforcement shear resisting mechanism and the axial compression force; the term V_{sj} corresponds to the possible retrofit contribution with CFRP or metal jackets and can be estimated according to Eq. (2) [11]

$$V_{sj} = \frac{A_j}{s} f_j \cdot h \cdot \cot\theta = \frac{A_j}{s} 0.004 E_j \cdot h \cdot \cot\theta \tag{2}$$

where h is the overall pier section dimension parallel to the applied shear force, f_j is the adopted design jacket stress level corresponding to a jacket strain of 0.004, A_j is the transverse section area of the jacket sheets spaced at distance s and inclined of the angle θ relative to the member axis. This condition is introduced to avoid large dilation strains and hence excessive degradation of the concrete, as well as to provide adequate safety against the possibility of jacket failure. Therefore, using Eq. (1) for both PO2 specimens retrofit, two strip layers of CFRP sheet were adopted with 0.117mm thickness by 100mm width and spaced at 100mm along each pier height in order to increase the shear capacity. This retrofit was doubled at the pier base for improving the concrete confinement and, therefore, the overall pier ductility.

5 CYCLIC TEST OF THE RETROFITTED SPECIMENS

The retrofitted piers have been tested following the same cyclic displacement history of the original specimens, but three additional cycles were performed with increased top displacement amplitude corresponding to 2.9%, 3.2% and 3.6% peak drift ratios. Results for both specimens are included in the following sections.

5.1 Pier PO2-N2-R1

The damage evolution during the experimental test of the retrofitted specimen PO2-N2 is illustrated in Figure 9, for the pier west side. For small amplitude cycles, corresponding to drift below 0.7%, first cracks about 0.1mm wide occurred (Figure 9a). In the subsequent cycles the crack widths increased and new cracks were also developed along the pier height. For 17mm top displacement (1.2% drift), the damage pattern shown in Figure 9b was mainly characterized by diagonal cracks in the interval zones between the CFRP strips. Shear damage continued to increase in the next cycles and, for 2.4% drift (Figure 9c), cracking was concentred at the pier base without visible damage on the CFRP sheets. Failure of some of the fibers at the base was audible from this stage on. During the last cycles for 33mm top displacement (2.4% drift) the cracks on the concrete and CFRP developed a little. Figure 10 shows the damage evolution on the pier internal faces also visualized during the test, in correspondence with the exterior damage, presented in Figure 9. When the CFRP strips collapsed at the pier base, for 2.4% drift, the interior cracks increased considerably, as shown in Figure 10d. In the last cycles, generalized damage became visible, with interior collapse of the walls and buckling of the longitudinal reinforcement (Figure 10d), that caused a fast reduction of the pier capacity as evidenced in the response diagrams included in Figure 12. The final damage stage is also shown in Fig. 11. As can be seen in Figures 9 - 12, the retrofitted specimen showed good behavior in comparison with the original one, exhibiting well distributed cracking along the CFRP spacing. The shear retrofit design, as used for this pier, showed excellent performance since the shear failure mechanism was prevented and the collapse was achieved after the CFRP failed at the pier base under a flexure mechanism that occurred further after the original specimen response. Figure 12 shows the comparison between the original and retrofitted pier, where about 40% increase of the top force is reached and about 100% more of the maximum displacement is obtained, without significant reduction of the resistant force.

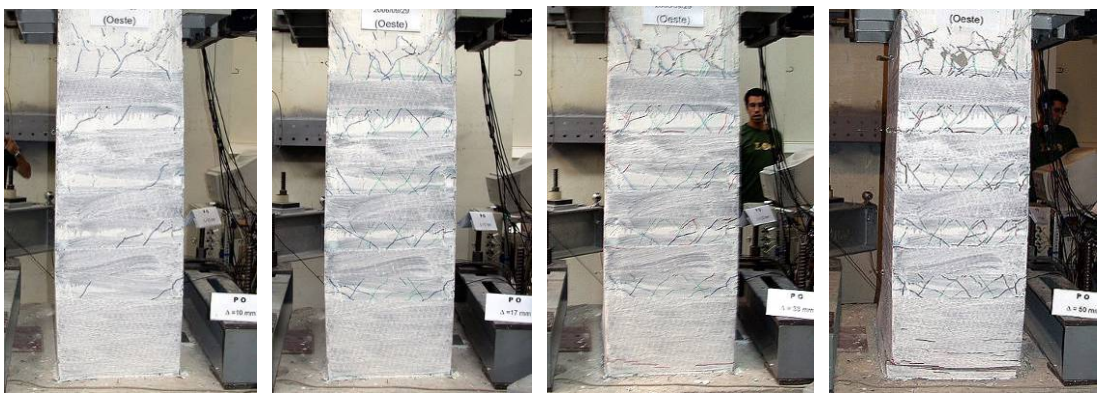

(a) 0.7% drift (b) 1.2% drift (c) 2.4% drift (d) 3.6% drift

Figure 9: Retrofitted pier PO2-N2. Damage from west side view during the test.

(a) 0.7% drift (b) 1.2% drift (c) 2.4% drift (d) 3.6% drift

Figure 10: Retrofitted pier PO2-N2 damage from internal east side view.

(a) East side (b) South side (c) West side (d) Internal and external

Figure 11: Final damage views of the retrofitted pier PO2-N2 corresponding to 3.6% drift ratio.

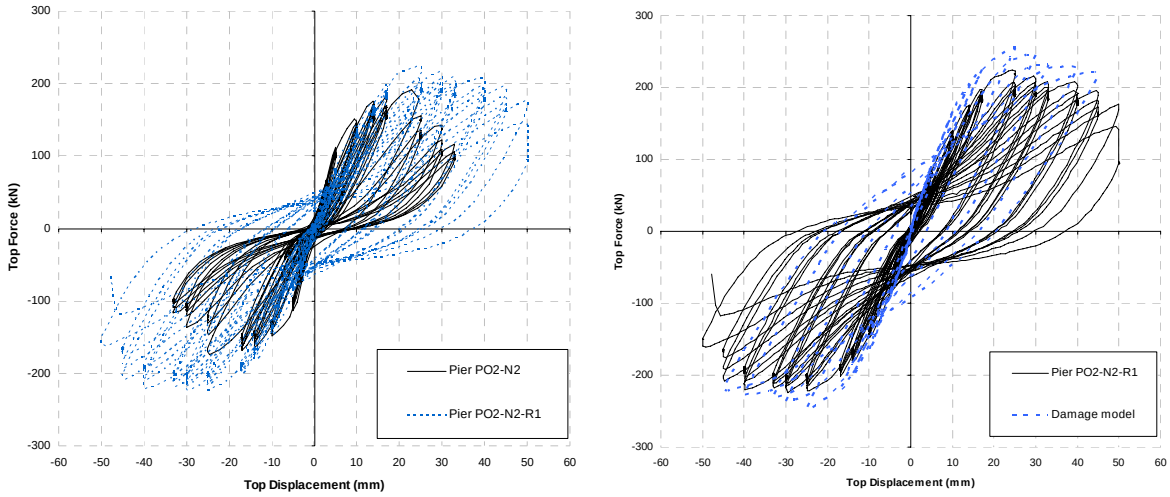

(a) PO2-N2 experimental curves before and after retrofit. (b) Numerical analysis for pier PO2-N2-R1

Figure 12: Experimental and numerical results comparison.

Figure 12b includes the comparison of numerical and experimental results for the test of PO2-N2-R1, in terms of top force-displacement response, showing that the numerical simulation model slightly overestimated the stiffness and peak strength of the specimen. Numerical simulations show also that compressive damage for 1.8% drift (Figures 13a and b) is greater than for the original pier because shear capacity increased by CFRP sheets and a flexure type deformation mode was activated. From the results illustrated in Figure 13e, it can be seen that a plastic hinge was formed, since red colors of the longitudinal bars are concentrated at the pier base; this fact agrees with the deformed mesh shown in Figure 13c. Although transverse steel has reached the yielding phase (Figure 13d), the CFRP sheets, simulated as high strength steel bars and shown in Figure 13f, are resisting well bellow the ultimate strength (about

3800MPa), avoiding the pier to exhibit a shear failure mode and, therefore, reducing shear deformation. In fact, this is the reason for the maximum flexural forces increase on the retrofit pier (see Figure 12), due to the greater number of longitudinal rebars having reached yielding.

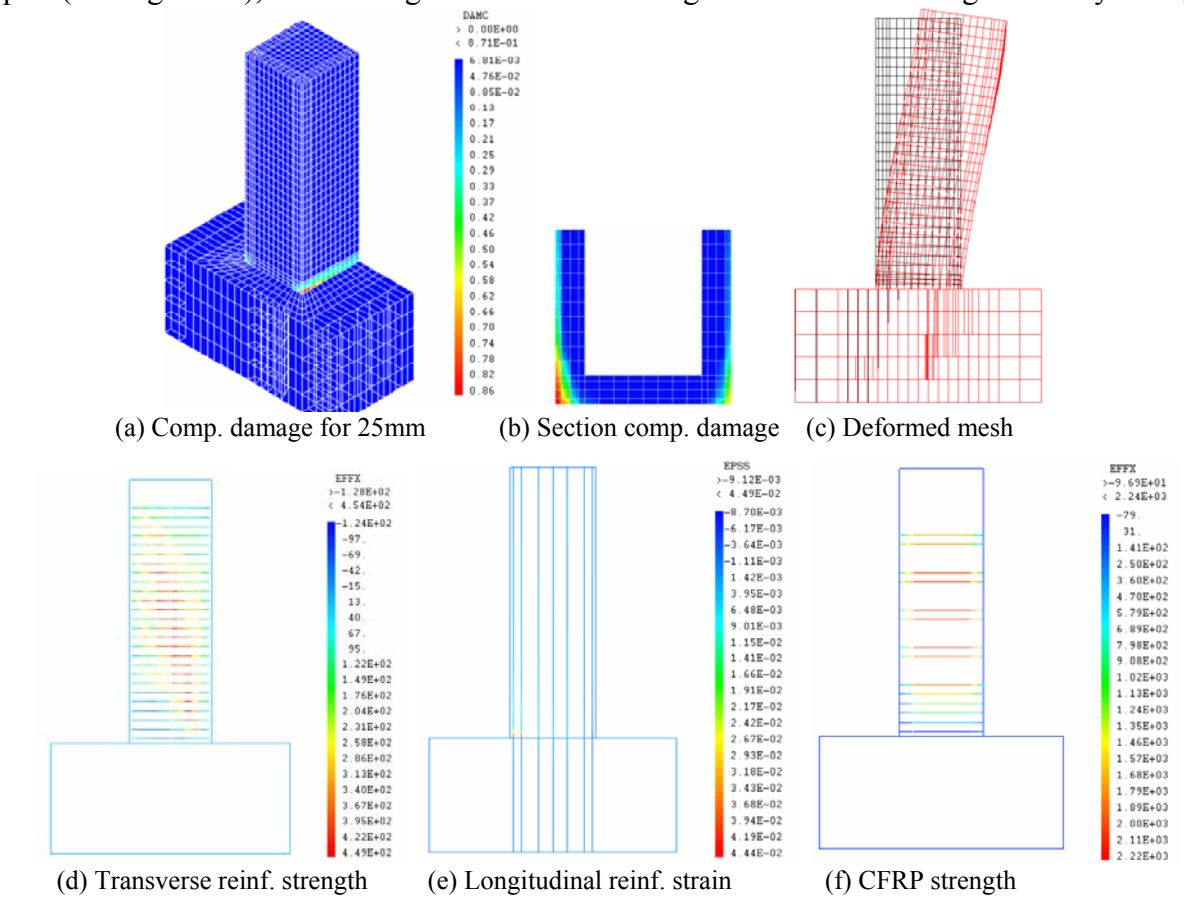

(a) Comp. damage for 25mm (b) Section comp. damage (c) Deformed mesh

(d) Transverse reinf. strength (e) Longitudinal reinf. strain (f) CFRP strength

Figure 13: Numerical results of PO2-N2-R1 for 1.8% drift.

5.2 Pier PO2-N3-R2

As referred before this pier was retrofit with transversal steel bars in the interior side near the base zone. The damage evolution during the experimental test of this specimen is illustrated in Figure 14, for the pier west side. As expected, for the first cycles, the damage observed was quite similar to the previous pier (PO2-N2-R1), until 2.4% drift was reached. The same pattern was observed for the 3.6% drift with an increase of crack opening at the base. At this stage it was possible to identify the failure mode based on a plastic hinge at the bottom. In the subsequent cycles, generalized damage became visible, with buckling of the longitudinal reinforcement, and crushing of the concrete (Figure 15) which caused gradual reduction of the pier capacity (Figure 16). However, for this case, buckling was observed in the outer rebars when the CFRP sheets lost the confinement capacity, whereas the retrofit with interior steel bars was quite effective in avoiding internal deformations.

As can be seen in Figures 14 and 15, this retrofitted specimen showed good behavior and relevant improvement in comparison with the other retrofitted one (PO2-N2-R1), mainly in terms of maximum displacement. Again the shear retrofit design provided excellent performance since the shear failure mechanism was prevented and the collapse was reached after longitudinal rebar failure and crushing of concrete (Figure 15b) for a very high level of top displacement under flexure mechanism. Figure 16 shows the comparison between the original and the two different retrofitted piers.

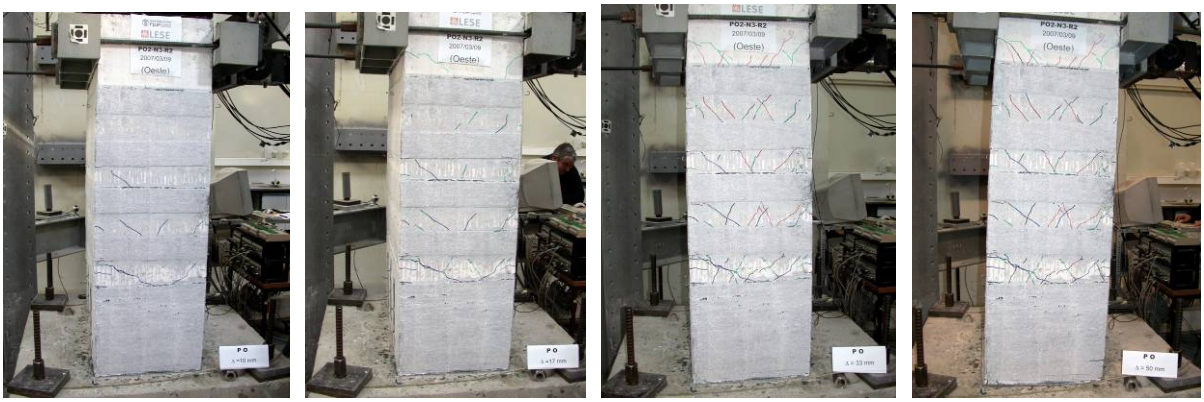

(a) 0.7% drift (b) 1.2% drift (c) 2.4% drift (d) 3.6% drift

Figure 14: Retrofitted pier PO2 damage from west side view.

(a) North side view (b) Local North side view (c) Este side view (d) Local Este side view

Figure 15: Final damage of the retrofitted pier PO2 corresponding to 3.6% drift ratio.

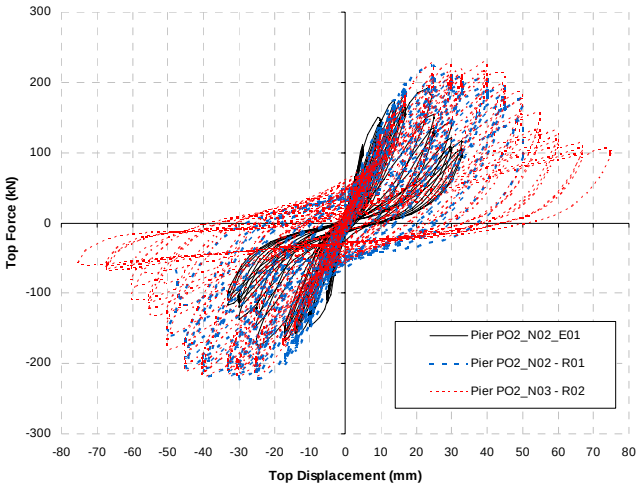

Figure 16: Experimental results comparisons of PO2 piers before and after retrofit with different confinement.

6 CONCLUSIONS

Original specimens evidenced that the collapse was achieved because of insufficient shear capacity. Cracks were observed at lateral sides (east and west faces), where the concrete cover crushed within the entire pier height and severe shear damage was observed with significant concrete degradation due lack of transverse reinforcement efficiency. As expected, higher initial stiffness and maximum forces were achieved for the pier with great axial load.

The numerical cyclic solution obtained with the damage model, agrees very well with the experimental results and the main aspects of the collapse mechanism were achieved satisfactorily. This numerical model, with several results of damage patterns and steel strain/stress,

allows to understand and confirm the importance of the shear deformation on the piers response.

The CFRP retrofit showed excellent benefits on the two pier behavior since it avoided the shear collapse and a flexure mechanism with plastic hinge at the pier base was achieved. In both piers, ultimate drift increased from 2.4% to 3.6%, with reasonable values of seismic capacity, and well distributed cracking was obtained. The adopted retrofitting strategy has evidenced good ability for the improvement of the seismic pier behavior both in ductility and strength.

The specimen retrofitted also in the interior side showed good increase of maximum displacement when compared with the other retrofitted one. The collapse was reached for a very large top displacement after failure of longitudinal reinforcement and crushing of concrete, this occurred when the CFRP sheets lost the confinement capacity and allowed rebar buckling in the outer face of the pier wall, while the interior transversal steel bars were still effective in avoiding internal rebar buckling.

7 ACKNOWLEDGEMENTS

The authors wish to acknowledge the "Irmãos Maia, Lda" company, for the construction of the tested piers and "S.T.A.P.- Reparação, Consolidação e Modificação de Estruturas, S. A." company for the repair and retrofit works. Final acknowledges to the laboratory staff, mainly Mr. Valdemar Luís, for all the care on the test preparation.

REFERENCES

[1] Rocha, P., et al. Seismic Retrofit of RC Frames. *Computers&Structures*, May, 2004

[2] Delgado, P., A. Costa, and R. Delgado Different Strategies for Seismic Assessment of Bridges – Comparative studies. *13th World Conference on Earthquake Engineering*, Vancouver, Canada, 1-6 August, 2004

[3] Delgado, P., et al. Experimental Tests on Seismic Retrofit of RC Piers. *100th Anniversary Earthquake Conference*, San Francisco, USA, 18-22 April, 2006

[4] Delgado, P., et al. Experimental Cyclic Tests and Retrofit of RC Hollow Piers. *13th European Conference on Earthquake Engineering*, Geneva, Switzerland, 3-8 September, 2006

[5] Pavese, A., D. Bolognini, and S. Peloso FRP seismic retrofit of RC square hollow section bridge piers. *Journal of Earthquake Engineering*, 2004

[6] CEA Manuel d'utilisation de Cast3m, Commissariat à l'Énergie Atomique. *Pasquet, P.*, 2003

[7] Faria, R., J. Oliver, and M. Cervera A strain based plastic viscous damage model for massive concrete structures. *International Journal of Solids and Structures*, 35(14), 1533-1558, 1998

[8] Costa, C., et al. Implementation of the Damage model in Tension and Compression with Plasticity in Cast3m. *Report EUR, ISPC, CEC, JRC, Ispra (VA), Itália*, (publication stage), 2005

[9] Faria, R., N.V. Pouca, and R. Delgado Simulation of the Cyclic Behaviour of R/C Rectangular Hollow Section Bridge Piers via a Detailed Numerical Model. *Journal of Earthquake Engineering*, 2004

[10] Giuffrè, A. and P. Pinto Il comportamento del cemento armato per sollecitazione ciclice di forte intensitá. *Giornale del Genio Civile*, 1970

[11] Priestley, M.J.N.S., F.; Calvi, G.M. *Seismic Design and Retrofit of Bridges*, New York, John Wiley & Sons, 1996